PHYSICAL REVIEW B VOLUME 56, NUMBER 16 15 OCTOBER 1997-II

Carrier-lifetime enhancement and mass discontinuity inferred from transport in a parabolic quantum well during subband depopulation

G. R. Facer, B. E. Kane, and R. G. Clark
National Pulsed Magnet Laboratory and Semiconductor Nanofabrication Facility, University of New South Wales, Sydney NSW 2052, Australia

L. N. Pfeiffer and K. W. West
Bell Laboratories, Lucent Technologies, Murray Hill, New Jersey 07974

(Received 24 June 1997)

In $GaAs/Al_xGa_{1-x}As$ parabolic quantum wells, subbands are depopulated by a magnetic field in the well plane. A small additional perpendicular field induces Shubnikov–de Haas (SdH) oscillations, which we have used to determine the carrier density, effective mass, and lifetime, throughout the two-subband-to-one-subband transition. The masses of carriers in the first and second subbands differ by 50% near the threshold of population of the second subband. The second subband SdH lifetime is enhanced near the threshold, even though the onset of two-subband transport increases the sample resistance. [S0163-1829(97)50340-7]

Electrons in a wide parabolic quantum well (WPQW) can manifest characteristics of three-, two-, and one-dimensional systems. Originally developed to produce a slab of 3D electrons in a high-mobility modulation-doped heterostructure,[1,2] WPQW's in fact confine a quasi-2D system, with typically two to four subbands occupied. A magnetic field $B_\parallel$ applied in the plane of the well depopulates the higher subbands, and also elongates and flattens the 2D electron Fermi surface along the axis perpendicular to $B_\parallel$. Electrons may consequently exhibit instabilities characteristic of 1D systems,[3] and superconductivity.[4]

The effects of $B_\parallel$ on electrons in a WPQW have been previously studied using transport,[5–7] capacitance,[8] far infrared,[9] and photoluminescence[10] techniques. The transport measurements in particular reveal structure associated with subband occupancy thresholds and a monotonic increase in resistance with $B_\parallel$ at high fields, when only the lowest subband is occupied. The electrons remain metallic for all values of $B_\parallel$, and consequently the resistance reveals little about the effect of $B_\parallel$ on the electrons in the PQW. A ''Fermi-surface probe'' would, therefore, be an important tool for elucidating the physics of electrons in a PQW in an in-plane field.

When the magnetic field is tilted away from the plane of the well, the allowed energies of the electrons become discrete[11] and Shubnikov–de-Haas (SdH) oscillations are observed in the magnetoresistance.[7,12] While at large tilt angles the resultant level spectrum is complex (the corresponding classical problem for a square well is chaotic[13]), at very small angles the level spectrum will approach a discretized replica of the density of states in a parallel field. Standard analysis of SdH oscillations induced by sufficiently small perpendicular fields ($B_\perp$) can thus, in principle, be used to determine subband occupancies, density of states, and carrier lifetimes of the system in a parallel field.

We have used this technique to study electrons in a WPQW in in-plane fields up to 12 T and at millikelvin temperatures, focussing in particular on the neighborhood of the second subband population threshold. We observe that the density of electrons in the second subband is well described by simple formulas for noninteracting electrons in a parabolic potential: there is no abrupt depopulation of the second subband, a phenomenon predicted[14] and reported[15] to occur in double layer systems as a consequence of the negative compressibility[16] of dilute 2D systems. We also observe a large (~50%) difference in the density of states of the two subbands near the threshold, in qualitative agreement with self-consistent calculations.[17] Most remarkably, we observe that the scattering time of electrons in the second subband *increases* as the subband is being depopulated, a probable consequence of the effectiveness of the electrons in the lowest subband in screening long-wavelength components of the disorder potential.

The Hamiltonian for electrons confined in an arbitrary potential $V(z)$ in a magnetic field with parallel and normal components $B_\parallel$ and $B_\perp$ is

$$H=\frac{1}{2m}\left\{\left[p_x+\frac{e}{c}zB_\parallel\right]^2+\left[p_y+\frac{e}{c}xB_\perp\right]^2+p_z^2\right\}+V(z)\,. \tag{1}$$

When $B_\perp=0$, both p_x and p_y commute with H, and the energies can be written

$$E(k_x,k_y)=\frac{\hbar^2}{2m_0}k_y^2+E_x(k_x)\,, \tag{2}$$

where E_x depends on the shape of $V(z)$ and on the magnitude of $B_\parallel$. The effect of $B_\parallel$ is to make $E(k_x,k_y)$ anisotropic.

When $B_\perp\neq 0$, the energy levels still have degeneracy $eB_\perp/hc$,[11,18] independent of the shape of $V(z)$ or the size of $B_\parallel$. The classical problem for a flat-bottomed well is chaotic for large $B_\perp/B_\parallel$.[13] If $B_\perp \ll B_\parallel$, however, $B_\perp$ will be a perturbation on the solutions in Eq. (2), i.e., a perturbation on a 2D electron system with anisotropic dispersion. The anisot-

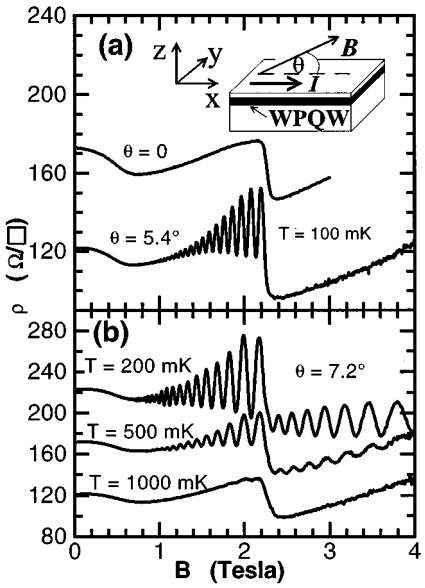

FIG. 1. (a) Magnetoresistivity traces for $\theta=0$ (upper curve, displaced upward by 50 Ω for clarity) and 5.5° (lower curve). Inset: WPQW sample, showing B tilt orientation. (b) Temperature dependence of the oscillations for a fixed tilt of 7.2°, again offset for clarity.

ropy can be described by $E_x(k_x)=\hbar^2k_x^2/2m_x$, and then the Landau-level spacings are simply

$$\delta E=\hbar\frac{eB_\perp}{c\sqrt{m_0m_x}} \tag{3}$$

(m_0 is the electron effective mass in bulk GaAs). This equation predicts that simple Landau-level structure will be observed at small tilt angles, and that the level spacing is sensitive (via m_x) to the shape of the confining potential $V(z)$. For a parabolic potential $V(z)=\frac{1}{2}m_0\Omega^2z^2$, the energy spacing can be solved explicitly,[19] and the mass dependence is described by

$$\sqrt{m_0m_x}=m_0\frac{\sqrt{\omega_c^2+\Omega^2}}{\Omega} \tag{4}$$

($\omega_c=eB_\parallel/m_0c$ is the cyclotron frequency). It is the quantity $\sqrt{m_0m_x}$ that is obtained from magnetoresistance measurements, through its influence on the density of states. Using noninteracting WPQW theory, measurement of the energy-level spacings can be used to determine the degree to which the electrons experience a parabolic potential.

The samples studied are GaAs/Al_xGa_{1-x}As heterostructures grown by molecular-beam epitaxy.[20] In the quantum-well region, the aluminium content x is varied quadratically between 0 and 0.3, creating a potential $\frac{1}{2}m_0\Omega^2z^2$ that is parabolic in the absence of any space charge [see inset to Fig. 1(a)]. Two Si δ layers, set back 400 Å from either side of the well, cause the well to be partially filled by a quasi-3D uniform slab of charge[1,6] ($N_{2D}=2.4\times10^{11}$ cm^{-2}). Three subbands are occupied at $B=0$ in our well, with densities similar to both experimental results and self-consistent calculations in other WPQW samples.[1,2,5] The zero-field electron sheet mobility in the WPQW at 4.2 K is 2.1×10^5 cm^2 V^{-1} s^{-1}. The calculated classical width of the 3D electron gas is ≈1100 Å.[21] The best results were obtained when the samples were not illuminated.

Figure 1 contains resistivity data as a function of B. In Fig. 1(a), the upper curve is the magnetoresistance for the case of a field precisely parallel to the sample plane (tilt angle $\theta=0$), offset upwards by 50 Ω for clarity. Up to 0.5 T, there is a poorly defined fall in resistivity associated with the depopulation of the third occupied subband. At 2.26 T, a sharp downward step in resistivity marks the depopulation of the second subband. Above this threshold $B_{\rm th}$, only the lowest electronic subband is occupied. Subband-related structure of this nature has been described extensively elsewhere.[1,5,7] When B is tilted slightly ($\theta\sim4°$), however, remarkably strong oscillations appear at fields approaching the depopulation threshold of the second subband. The lower trace in Fig. 1(a) shows data for $\theta=5.5°$. As the tilt increases ($\theta\gtrsim6°$), longer-period oscillations begin to appear where only one subband is occupied. For $\theta\gtrsim10°$, the peaks become irregular, and the results approach the form observed by Shayegan *et al.*[12] For all tilt angles, the oscillations are strongest in the region where two subbands are occupied and the occupancy of the second subband is low.

In Fig. 1(b) $\theta=7.2°$; the three traces were taken at sample temperatures of 200, 500, and 1000 mK as marked. At $T\sim1$ K, the strong oscillations are almost entirely gone, leaving only the more robust subband depopulation features.

Figure 2(a) shows oscillation index vs $1/B$, for $\theta=7.2°$, where only one subband is occupied. We assign sequential ''index'' labels to the oscillations (half-integer indices for maxima, integers for minima). It is clear that the oscillations have a SdH-type nature.

Peak and valley separations of the strong oscillations at $B<B_{\rm th}$ increase linearly with tilt angle, as does the separation between threshold and the first minimum [Fig. 1(b)]. The strong oscillations are, therefore, well explained by attributing them to SdH oscillations from the second subband, if the second subband population increases continuously from zero for $B<B_{\rm th}$.

The fact that the Landau-level degeneracy is $eB_\perp/hc$ enables us to determine densities (N_1 and N_2 in the lowest- and second-lowest subbands, respectively) simply by counting the strong oscillations below $B=B_{\rm th}$ (assuming $N_1=0$ at threshold, and that only two subbands are occupied above $B_\parallel=0.5$ T). That the density determined in this manner does not depend on $B_\perp$ is shown in Fig. 2(c), where index$\times\theta$ is plotted for seven angles ($3.6°<\theta<7.2°$): all data fall on a common curve. Figure 3(a) shows the electron sheet density results for the first and second subbands.

Density profiles in the subbands have been analyzed on the basis of previous predictions for the density of states (DOS) of noninteracting electrons in a parabolic well, where the DOS is subband independent.[11,18,19] Since the subband separation is $\hbar\sqrt{\omega_c^2+\Omega^2}$, the difference in density N_1-N_2 between the lower and upper subbands in a parabolic well is [from Eq. (4)]

$$N_1-N_2=\frac{m_0}{\pi\hbar}\frac{\omega_c^2+\Omega^2}{\Omega}. \tag{5}$$

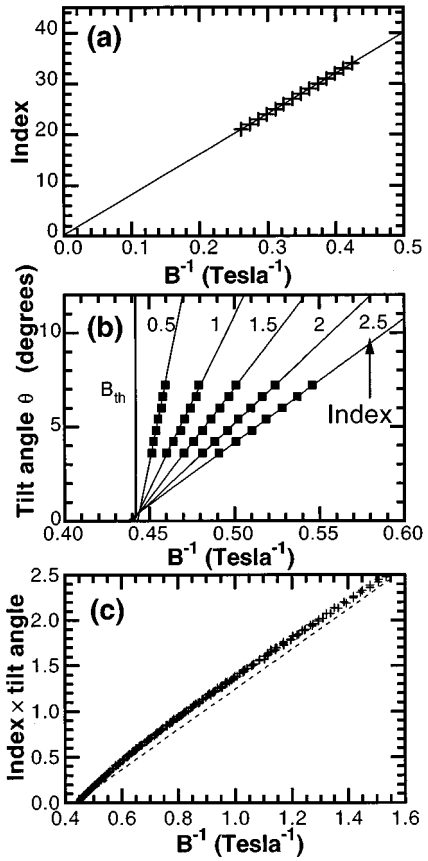

FIG. 2. Summary of magnetoresistance oscillation data. (a) Lowest-subband oscillation indices for $\theta=7.2°$, as a function of $1/B$. The dashed line is fitted to the index data points; (b) evolution of particular index positions with tilt angle (maxima have half-integer indices). Also shown (vertical line) is the subband depopulation threshold $B_{\rm th}$, to which the index positons converge. (c) Second-subband oscillation index scaled by θ. Note that the common curve is nonlinear.

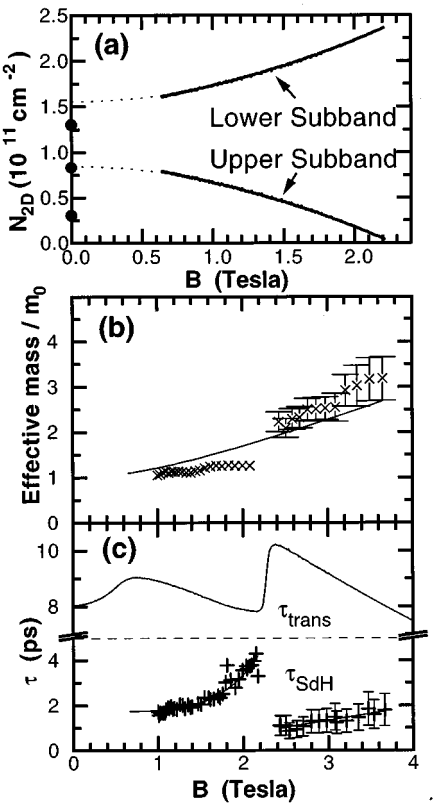

FIG. 3. Electron properties in the WPQW, as a function of electric field: (a) Electron sheet densities in the lowest- and second-lowest subbands; circles at $B_x=0$ are from fast Fourier transform data where $B\|z$. (b) Electron effective mass, normalized such that the effective mass in GaAs ($0.067m_e$) corresponds to 1; (c) electron scattering times—$\tau_{\rm SdH}$ derived from SdH data and the mobility-determined scattering lifetime $\tau_{\rm trans}$.

Equation (5) was fitted to the N_1 data, using Ω as the only adjustable parameter.[22] The N_1 fit gives the dotted lines in Fig. 3(a), and a value for Ω of $\hbar\Omega_{\rm fit}=2.6$ meV, differing from that obtained from the well growth parameters ($\hbar\Omega_{\rm gr}=6.3$ meV),[21] indicating that the electrons in the well are acting to diminish the depth of the well. This screening of the growth potential is consistent with other experimental studies of WPQW's.[1,2] Extrapolations of fitted densities to zero parallel field in Fig. 3(a) can be compared with results from spectral analysis of perpendicular-field data (filled circles); the N_2 results agree well, while the N_1 subtraction must be modified for $B<0.5$ T to take the third, sparsely occupied, subband into account ($N_{\rm third}\approx 3\times10^{10}$ cm^{-2}).

Further investigation of the density of states was carried out via field-dependent calculations of the effective carrier mass. At a fixed tilt angle, the temperature dependence of the strong SdH oscillation strengths can be used to determine the effective carrier mass $m^*=\sqrt{m_0 m_x}$ in the WPQW as a function of B.[23] The mass results calculated to first order are shown in Fig. 3(b). A value of one on the mass scale corresponds to m_0. The mass increases gradually from around $m^*=1$ at low fields until the depopulation threshold of the second subband. At the threshold field, the mass jumps upward by a factor $\approx$1.5, and thereafter increases smoothly, but more rapidly than in the two-occupied-subband region. It should be noted that as the calculations are based on the strong oscillations, the results pertain only to the subband from which the oscillations arise. At larger angles, first-subband oscillations become discernible at $B<B_{\rm th}$, but could not be used for reliable analysis. The solid line in Fig. 3(b) is calculated using the formula in Eq. (4), with $\Omega=\Omega_{\rm fit}$ from the density fitting given earlier. A different curvature is seen in the data than is predicted by the model. There is also no prediction of the discontinuity at $B=B_{\rm th}$ by the noninteracting-electron PQW theory.

When interactions are considered, a plausible explanation of the effective mass data develops: the potential profile experienced by electrons in different subbands differs qualitatively. While the upper subband electrons see an essentially parabolic potential, electrons in the lower subband interact to give a flatter-bottomed well profile. As the magnetic length (varying inversely with density) becomes much less than the well width, the electrons are only marginally influenced by the parabolic well edges. For the majority of the time, electrons in the highly occupied lower subband experience only the flat net potential across the bottom of the well. Approximate perturbative calculations show that the field dependence of the DOS in more square wells is subband dependent, whereas that for a parabolic well is not. Indeed, the sign

of the calculated lowest-subband DOS correction is different for the two well types, consistent with the jump in the data from below to above the noninteracting WPQW model, shown in Fig. 3(b).

Especially in the lower subband, self-consistent calculations for a PQW subject to parallel fields indicate that the k_x dependence of dispersion is flatter, yielding a greater DOS.[17] A simple DOS calculation for a ''high-field limit'' of a flat-bottomed well similarly indicates that the electrons occupy a well with a profile between the extremes of square and parabola.

Using the field-dependent mass obtained above and resistivity amplitudes as a function of θ, the lifetimes τ_{SdH} associated with the SdH oscillations were calculated. This calculation was again performed using a standard SdH model[23] to first order. The τ_{SdH} results are shown in Fig. 3(c). Not surprisingly, there is a discontinuity in the calculated scattering times where the second subband is depopulated. The greater lifetime in the second subband suggests the possibility of screening of scattering centers by electrons in the heavily occupied lowest subband. The high strength of the oscillations at fields slightly below the second subband depopulation step manifests as a greatly increased value of τ_{SdH}. Even the highest observed τ_{SdH}, however, is still considerably smaller than the mobility-determined scattering time τ_{trans}, which is also given in Fig. 3(c).

It is not clear why scattering should be so suppressed in a barely occupied subband, although similar results have been observed in other two-subband systems.[24] An increasing τ_{SdH} is necessary to explain the strength of the oscillations near threshold. Models in which only the mass changes do not fit the data. It should be emphasized that the τ_{SdH} determination is selective of electrons in the upper subband, and hence there is no conflict with the observed gradual increase in total resistivity for $\theta=0$. As a check on the first-order approximation used throughout, the second term was calculated for $\theta=4.8°$, and found to have a negligible effect on the modelling result.

A Dingle ratio $R_d=\tau_{\mathrm{trans}}/\tau_{\mathrm{SdH}}$ greater than unity has also been observed in high-mobility two-dimensional systems, both in GaAs (Ref. 24) and $Si_{1-x}Ge_x$[25] heterostructures. Furthermore, that $R_d>1$ provides insight into the nature of scattering processes in the well: most scattering events in the WPQW involve only a small change in the carrier momentum. Carrier mobilities are less strongly influenced than SdH oscillations by scattering events with small collision wave vectors k_s. This is because several such events are required to effectively randomize the electron momentum, whereas the coherence required for SdH oscillations is fragile even to small k_s. $\tau_{\mathrm{trans}}/\tau_{\mathrm{SdH}}$ in our experiment ranges between 4 and 10. We can, therefore, conclude that a majority of scattering events in the WPQW are caused by long-wavelength fluctuations. Interestingly, small-angle scattering events are not conventionally expected to dominate in WPQW structures. The fact that mobilities in WPQW's are significantly less than in the best two-dimensional systems has traditionally been explained in terms of alloy disorder in the well region, whereas long-wavelength potential fluctuations are more characteristic of remote impurity effects.

A preponderance of small-angle scattering events in the WPQW also explains why resistivity in the upper subbands is higher than in the lowest subband. With $N_2<N_1$, the Fermi wave vector in the second subband is smaller, so the small k_s now significantly alters the electron momentum. As the carrier momentum is more easily randomized, the resistivity in the upper subband is relatively high, accounting for the dramatic step in overall resistivity at B_{th}. Predictions of scattering times in different subbands do exist,[26] but for δ-function scatterers within the well region. These local scatterer calculations do qualitatively agree with the τ_{SdH} discontinuity between subbands, but do not go into sufficient detail on field dependences to distinguish short- from long-range fluctuations.

We conclude that scattering in the WPQW is dominated by small-angle scattering events, probably due to remote impurities. The corollary of this result is that the quasi-3D electron system screens local scatterers with a thoroughness not previously anticipated. With a practical method now available for characterizing electrons in particular subbands, it is anticipated that examining WPQW's with more than two clearly resolvable occupied subbands will yield further valuable information on 3D electron systems.

We thank Ross McKenzie for valuable discussions. This work was supported by the Australian Research Council (Grant No. A69700583).

[1] M. Shayegan *et al.*, Surf. Sci. **229**, 83 (1990).
[2] A. Wixforth *et al.*, Surf. Sci. **228**, 489 (1990).
[3] L. Brey and B. I. Halperin, Phys. Rev. B **40**, 11 634 (1989).
[4] M. Rasolt and Z. Tesanovic, Rev. Mod. Phys. **64**, 709 (1992).
[5] E. G. Gwinn *et al.*, Phys. Rev. B **39**, R6260 (1989).
[6] T. Sajoto *et al.*, J. Vac. Sci. Technol. B **7**, 311 (1989).
[7] K. Ensslin *et al.*, Phys. Rev. B **47**, 1366 (1993).
[8] M. Sundaram, K. Ensslin, A. Wixforth, and A. Gossard, Superlattices Microstruct. **10**, 157 (1991).
[9] K. Karrai *et al.*, Phys. Rev. Lett. **67**, 3428 (1991).
[10] M. Fritze *et al.*, Phys. Rev. B **48**, 15 103 (1993).
[11] L. Smrčka, J. Phys.: Condens. Matter **2**, 8337 (1990).
[12] M. Shayegan *et al.*, Phys. Rev. B **40**, R3476 (1989).
[13] T. M. Fromhold *et al.*, Phys. Rev. Lett. **75**, 1142 (1995).
[14] P. P. Ruden and Z. Wu, Appl. Phys. Lett. **59**, 2165 (1991).
[15] Y. Katayama *et al.*, Phys. Rev. B **52**, 14 817 (1995).
[16] J. P. Eisenstein, L. N. Pfeiffer, and K. W. West, Phys. Rev. Lett. **68**, 674 (1992).
[17] M. P. Stopa and S. Das Sarma, Phys. Rev. B **40**, R10 048 (1989).
[18] R. Merlin, Solid State Commun. **64**, 99 (1987).
[19] J. C. Maan, in *Two Dimensional Systems, Heterostructures and Superlattices*, edited by G. Bauer, F. Kuchar, and H. Heinrich (Springer-Verlag, Berlin, 1984), p. 183.
[20] L. N. Pfeiffer, K. W. West, H. L. Stormer, and K. W. Baldwin, Appl. Phys. Lett. **55**, 1888 (1989).
[21] B. E. Kane *et al.* (unpublished).
[22] Numerically, the best possible fit to the data is hyperbolic in form $N_1=\sqrt{(8.06B\times10^{14})^2+(1.53\times10^{15})^2}$.
[23] A. Isihara and L. Smrčka, J. Phys. C **19**, 6777 (1986).
[24] T. P. Smith III, F. F. Fang, U. Meirav, and M. Heiblum, Phys. Rev. B **38**, R12 744 (1988).
[25] D. Monroe *et al.*, J. Vac. Sci. Technol. B **11**, 1731 (1993).
[26] H. Tang and P. N. Butcher, J. Phys. C **21**, 3313 (1988).